ISTITUTO NAZIONALE DI GEOFISICA E VULCANOLOGIA

Site characterization report at the seismic station IT.PZI1 – Pizzoli, L'Aquila (AQ)

Report di caratterizzazione di sito presso la stazione sismica IT.PZI1 – Pizzoli, L'Aquila (AQ)

Working Group

Geology: Deborah DI NACCIO[1]

Geophysics: Giuseppe DI GIULIO[1], Maurizio VASSALLO[1], Michele FONDRIEST[2]

(1) Istituto Nazionale di Geofisica e Vulcanologia

(2) ISTerre - Université Grenoble Alpes

Date: December 2021

Subject: **Final report illustrating the site characterization for seismic station IT.PZI1**

Convenzione DPC-INGV 2019-21, All.B2- WP1, Task 2: "Caratterizzazione siti accelerometrici" (Coord.: G.Cultrera, F. Pacor)
Cite as: Working group INGV "Agreement DPC-INGV 2019-21, All.B2- WP1, Task 2", (2021). Geological report at the seismic station *IT.PZI1 – Pizzoli* http://hdl.handle.net/2122/15053

INDEX

INTRODUCTION

In this report we present the geological setting, geophysical measurements and the results obtained in the framework of the 2019-2021 agreement between INGV and DPC, called *Allegato B2: Obiettivo 1 - TASK 2: Caratterizzazione siti accelerometrici (Responsabili: G. Cultrera, F. Pacor)* for the site characterization of station IT.PZI1 (Pizzoli, L'Aquila).

Location and coordinates are reported in Table 1.

Table 1.

CODE	NAME	LAT [°]	LON [°]	ELEVATION [m]
IT.PZI1	PIZZOLI - 67017 L'AQUILA	42.4356*	13.3262*	908*
ADDRESS	Via dell'Acquedotto di Pile, Colle, Marruci, Pizzoli, L'Aquila, Abruzzo, 67017, Italy			

* Coordinates from ITACA (Nov. 2021)

A. Geological setting

A1. TOPOGRAPHIC AND GEOLOGICAL INFORMATION

The topographic information is reported in Table 2. Table 3 summarizes the geological maps available in the literature and collected for the geological analyses in the site.

Table 2.

Topography	Description	Topography Class	Morphology Class	EC8 Class
	Flat surfaces, isolated slope, and reliefs with slope i<=15°	T1	P*	B

*Reference table from ITACA (March 2019)

Table 3.

Geological map	Source	Scale
IT.PZI1	Geological map of Italy sheets 139 (L'Aquila).	1:100.000
IT.PZI1	Carta Geologica d'Abruzzo (Vezzani & Ghisetti, 1998).	1:100.000
IT.PZI1	Carta geologica dei bacini della Laga e del Cellino e dei rilievi carbonatici circostanti (Marche meridionali, Lazio nord-orientale, Abruzzo settentrionale (Centamore et al., 1991).	1:100.000
IT.PZI1	Carta geomorfologica dei comuni Barete-Pizzoli (AQ) Table 2. (FAC-Ridefinizione delle Zone di Attenzione delle Faglie Attive e Capaci emerse dagli studi di microzonazione sismica effettuati nel territorio dei Centri abitati di Barete e Pizzoli in provincia de L'Aquila, interessati dagli eventi sismici verificatisi a far data dal 24 agosto 2016, 2021).	1:5.000
IT.PZI1	Carta Geologica-Tecnica (Microzonazione Sismica di Livello 3 del comune di Pizzoli-AQ, Regione Abruzzo, 2018).	1:5.000

In Table 4, Geological and Lithotechnical Units (according to Seismic Microzonation classification; Technical Commission SM, 2015) are described and are concerned to maps of following chapters. The term “original” means the result comes from preexisting cartography (Table 3); the term “deduced” means the result comes from an interpretation of preexisting cartography according to the nomenclature of corresponding cartography.

Table 4

GEOLOGICAL UNITS		**LITHOTECHNICAL UNITS**	
“Carta geomorfologica dei comuni Barete-Pizzoli (AQ). at 1:5:000 – FAC” (Table 2) *original*		(MZS) *deduced*	
code	**description**	**code**	**description**
Oloa1	Active complex slope instability	Oloa1	Slope instability materials
Olob1	Eluvial-colluvial deposits	GMec	Gravel, a mixture of gravel, sand, and silt
Olob2	Alluvial fan deposits	GMca	Gravel, a mixture of gravel, sand, and silt
AVMa3	Alluvial scree materials	GM	Gravel, a mixture of gravel, sand, and silt
AVM8 b	Alluvial fan deposits	GMca	Gravel, a mixture of gravel, sand, and silt
RMOb	Alluvial deposits	GRfd	Cemented granular rock
Masa	Very intensely fractured rocks	LPS	Very intensely fractured rock
Masb	Carbonate geological bedrock	SFLP	Layered geological bedrock

A2. GEOLOGICAL MAP

Figure 1 reports the Geological Map in a 1kmx1Km square area around the station.

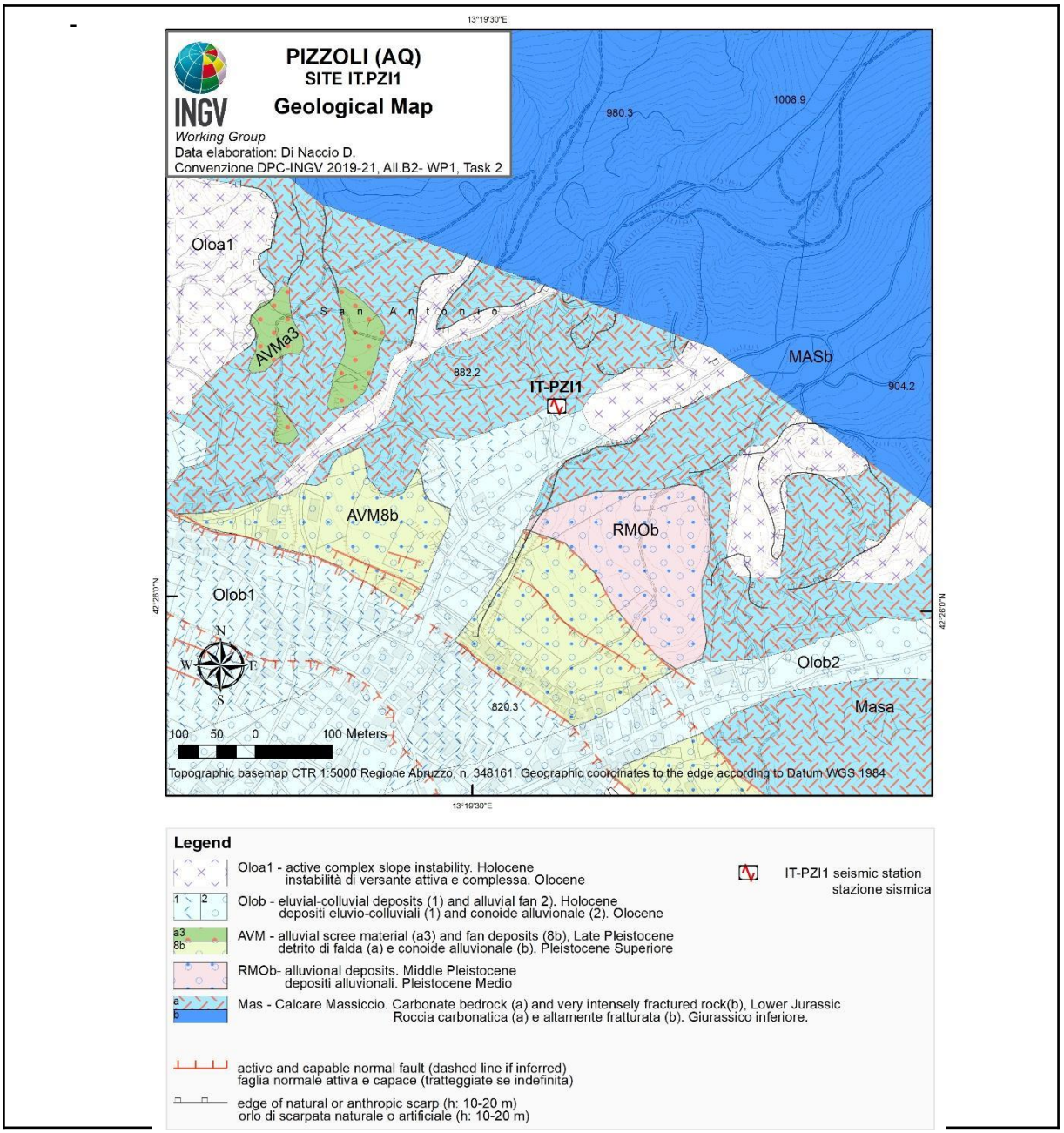

Figure 1. Geological map of seismic station IT.PZI1. Scale 1:5.000. Geological units come from "Carta geomorfologica dei comuni Barete-Pizzoli (AQ), Table 2 at 1:5.000 (FAC-Ridefinizione delle Zone di Attenzione delle Faglie Attive e Capaci emerse dagli studi di microzonazione sismica effettuati nel territorio dei Centri abitati di Barete e Pizzoli in provincia de L'Aquila, interessati dagli eventi sismici verificatisi a far data dal 24 agosto 2016, 2021)".

A3. LITHOTECHNICAL MAP

Figure 2 reports the Lithotechnical Map in a 1kmx1Km square around the station.

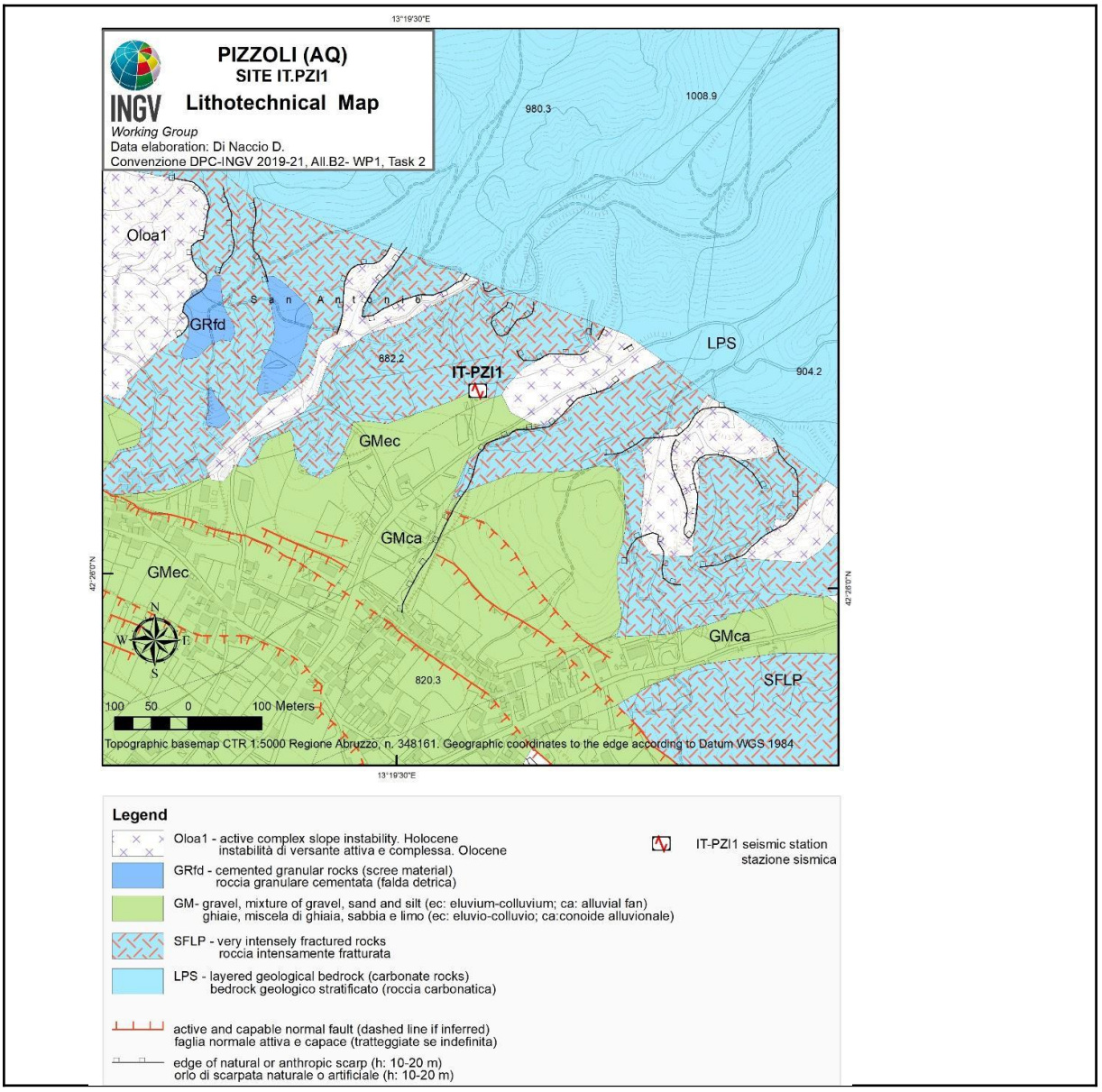

Figure 2. Lithotechnical map of the seismic station IT.PZI1. Scale 1:5.000. The lithotechnical units are from the "Carta geomorfologica dei comuni Barete-Pizzoli (AQ), Table 2 at 1:5.000 (FAC-Ridefinizione delle Zone di Attenzione delle Faglie Attive e Capaci emerse dagli studi di microzonazione sismica effettuati nel territorio dei Centri abitati di Barete e Pizzoli in provincia de L'Aquila, interessati dagli eventi sismici verificatisi a far data dal 24 agosto 2016, 2021)" and assigned according to the nomenclature of Seismic Microzonation (Technical Commission SM, 2015).

A4. SURVEY MAP

Figure 3 is the Survey Map reporting the investigations and geophysical surveys conducted by the INGV Working Group.

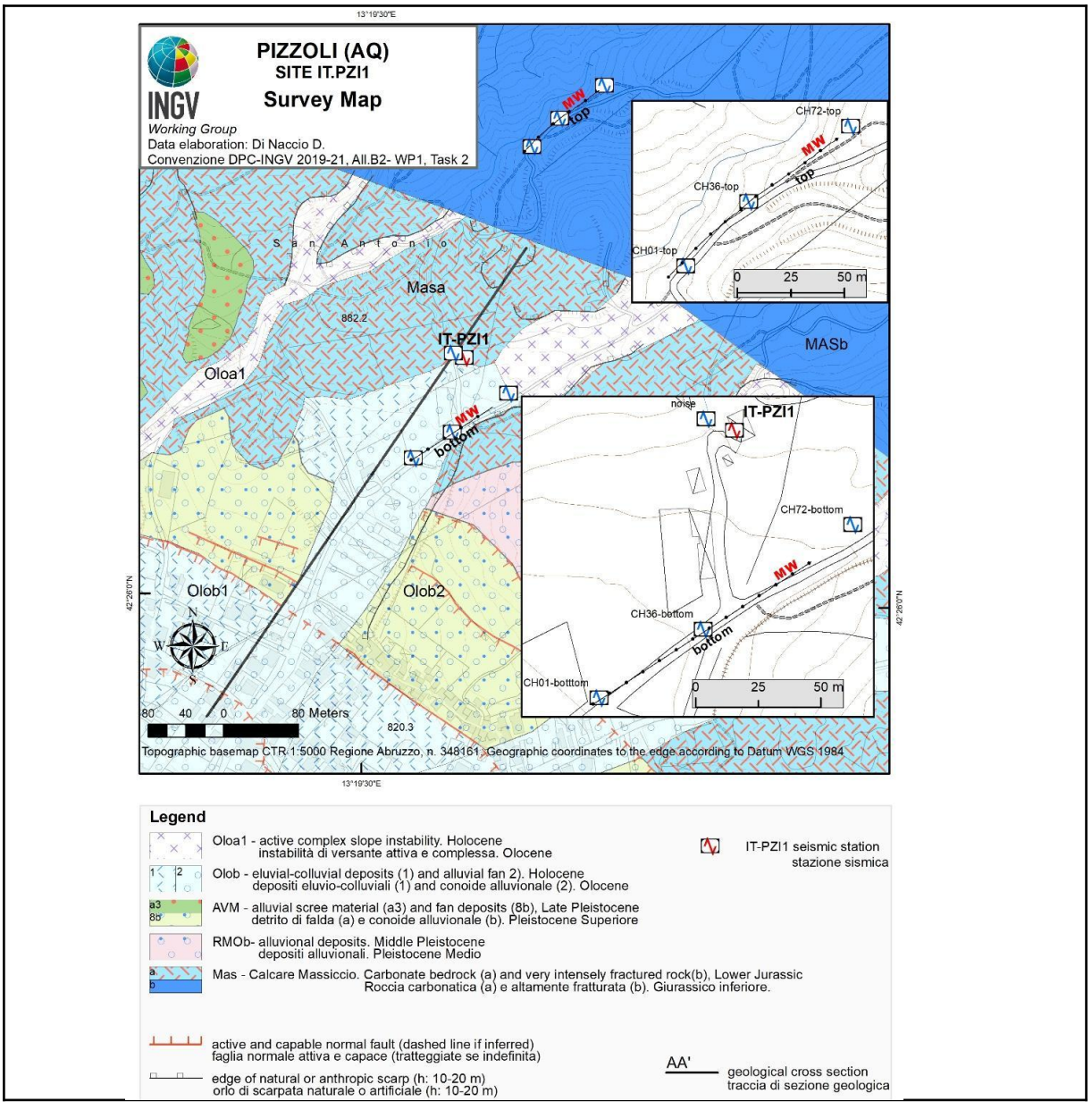

Figure 3. Map of the surveys in the surroundings of the IT.PZI1 seismic station. Scale 1:5.000. The maps at the right contain details of the geophysical survey conducted by the INGV Working Group for the seismic characterization of the site (Agreement DPC-INGV 2019-21, All. B2, WP1 - TASK 2). Refer also to part B "Vs profile" in this report.

A5. GEOLOGICAL MODEL

5.1 General description

The seismic station is located on the axial portion of the central Apennine chain undergoing regional uplift and NE-SW active extension since Late Neogene-Early Quaternary (Carafa and Bird, 2016). Extension at 2.5-3.5 mm/a (Carafa and al. 2020; Devoti et al. 2017) shaped a complex landscape featuring previous thrust-belt ranges, fluvial landforms, karst plateaus, and fluviolacustrine basins. NW-SE and NNW-SSE striking normal faults dissect and overprint older compressional features, drive the deposition in intramountain basins and control the Late Pleistocene (< 126 ka)-Holocene continental deposits and landforms. In the studied area the SW-dipping Pettino fault bounds the eastern Upper Middle Aterno basin striking in the NW-SE direction roughly parallel to the elongation of Mt. Marine. The seismic station is placed at the footwall where the Calcare Massiccio Fm. (Lower Jurassic; LPS in Figure 2) is highly deformed and fractured. The cataclastic zone is about 50m wide (SFLP in Figure 2). At the hanging wall, the alluvial and slope Quaternary continental deposits (OLOb, AVM and RMOb in Figure 2) fill the tectonic basin. A Late Quaternary activity of the fault is supported by dislocated and faulted Late Pleistocene alluvional and slope deposits, geomorphic evidence including fault scarp exposure, triangular facets and paleoseismological evidence of past-earthquakes (Blumetti, 1995; Galadini e Galli, 2000; Moro et al., 2002; Galli et al., 2011, Moro et al., 2016). For these characteristics the Pizzoli fault is considered active and capable.

5.2 Geological Section

The NE-SW-oriented geological cross section (black line in the Figure 3 and Figure 4) accompanying geological survey map provides an interpretation of the third dimension. It is based on the extrapolation of surface data with pre-existing geological and structural studies, geophysical investigations and the determined seismic velocities profiles (see part B of this report) as well as data from other subsurface sources.

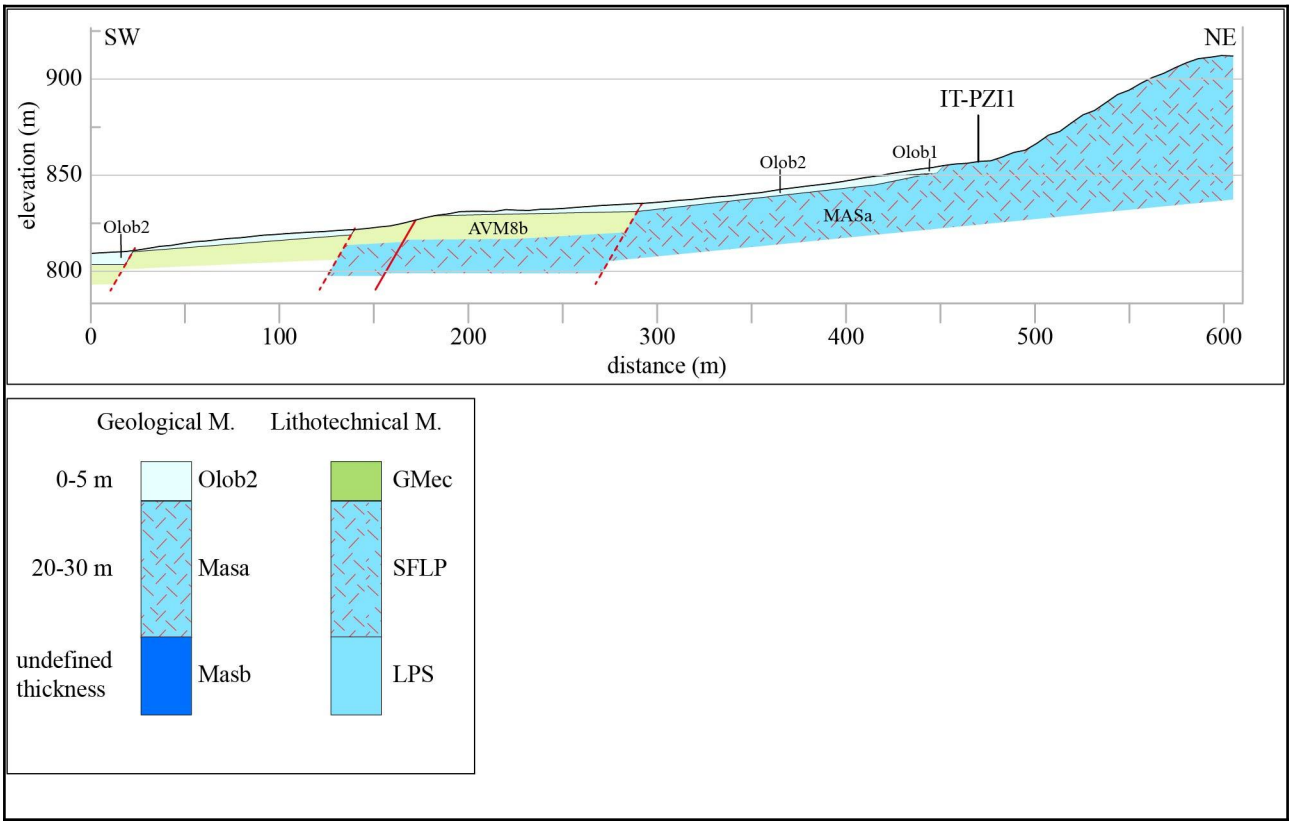

Figure 4. Top: Geological section across IT.PZ1 seismic station (see Figure 3 for location). Bottom: subsoil model for the site. See Figure 1 and 2 for symbology

5.3 Subsoil model

The subsoil model is based on surface and subsurface geological and geophysical observations and the determined seismic velocities profiles (see part B of this report).

The lithotecnical units considered representative of the site around the IT-PZI1-seismic station (Figures 1-2 and Table 4) are the following:

SFLP: very high fractured and deformed rocks of the Pizzoli cataclastic zone. The thickness is of 20-40 m

LPS: the carbonatic rocks of the Calcare massiccio Fm. which represents the geological bedrock.

GMec: a thin layer (0-5m) of colluvium-eluvium (GMec) mainly consisting of gravel and mixture of sand and silt can cover the SFLP unit.

B. Vs profile

B1. GEOPHYSICAL INVESTIGATIONS

In this part of the report, we present the geophysical surveys carried out for the seismic characterization of the IT.PZI1 station.

This sector of Pizzoli is characterized by Monte Marine fault zone, and because a previous seismic station (IT.PZI) was working up to 2013-10-14, geophysical surveys investigated a wide area surrounding IT.PZI1 (Figure 5).

IT.PZI was set at a distance of about 100 m far and with a lower elevation (908 m a.s.l versus 941 m, respectively) with respect to the previous station IT.PZI1. Figure 5 shows the target area with locations of the geophysical experiments; a zoomed view is shown in Fig. 6.

Geophysical surveys are based on two linear arrays of 72 vertical geophones (Geospace with eigen-frequency of 4.5 Hz) connected by means of three multichannels modules (Geode by Geometrics). The spacing between adjacent geophones was set equal to 1.5 m, for a total length of each linear array of 106.5 m. As an active source, we acquired the seismic signals produced by the vertical impact of a 5 kg hammer on a metal plate set on the ground (MASW surveys). The shots were made along the MASW line at distances of -10 m, -5m, -1m, 53.25m, 107.5m and 116.5 m from the first geophone (which is considered at a position of 0 m). For each shot-point position, the measurements were repeated from 2 to 4 times in order to increase the signal-to-noise ratio. Seismic active data were acquired by the Geode multichannels system with a sampling rate of 0.125 ms for a duration of 2 s. We refer to the two MASW arrays as top and bottom MASW (Fig. 5). Pictures of the top (a and b) and bottom (c and d) MASW lines are illustrated in Fig. 7.

We also acquired passive data at each linear array (using the same equipment of the active survey) through 15 time windows of 240 s length (4 minutes) at a sampling rate of 4 ms. Because the bottom MASW is very close to IT.PZI1 station (Fig. 6), we focus more on this survey in the next part of the report. The bottom MASW line is at about 50 m far IT.PZI1.

Several ambient-vibration measurements (or noise) were also performed using seismic three-components velocimeters along the two linear arrays (red marker in Fig.s 5 and 6). Specifically, we used digitizers (Reftek130) coupled to Lennartz velocimeters (Le3d5s with eigen-frequency of 0.2 Hz) that recorded noise data at least for 1 hour. Noise measurements were carried out approximately at the begin, middle and end positions of the top and bottom MASW (see Fig. 5 and 6). A further vibration measurement was carried out very close to IT.PZI1 (i.e. 10 m far; named 'noise' in Fig. 6). The housing of IT.PZI1 is a cabinet with presence

of water pumps; housing with the closest ''noise'' measurements is shown in Fig. 8. This 'noise' measurement was carried out on the 19th May of 2021 (cloudy day), whereas the top and bottom MASW (together with the CH noise data of Fig. 5) were recorded on the 18th and 19th August of 2020, respectively (very sunny days and no wind).

To assess the resonant frequency (f0) of the site, the horizontal-to-vertical (H/V) spectral analysis has been calculated. Using surface-wave and cross-correlation analysis based on array techniques, we provide results also in terms of dispersion curves (DC). The observed curves were inverted to obtain the shear-wave velocity (Vs) profiles for the studied area. The obtained velocity models are suitable for determination of the average Vs velocity in the uppermost 30 m (Vs30) and assigning then the soil class category as prescribed by current Italian seismic code (NTC18) and Eurocode (EC08).

The software of analysis was *Geopsy* (http://www.geopsy.org; Wathelet et al. 2020) together with ad-hoc code to perform the cross-correlation analysis (Vassallo et al. 2019).

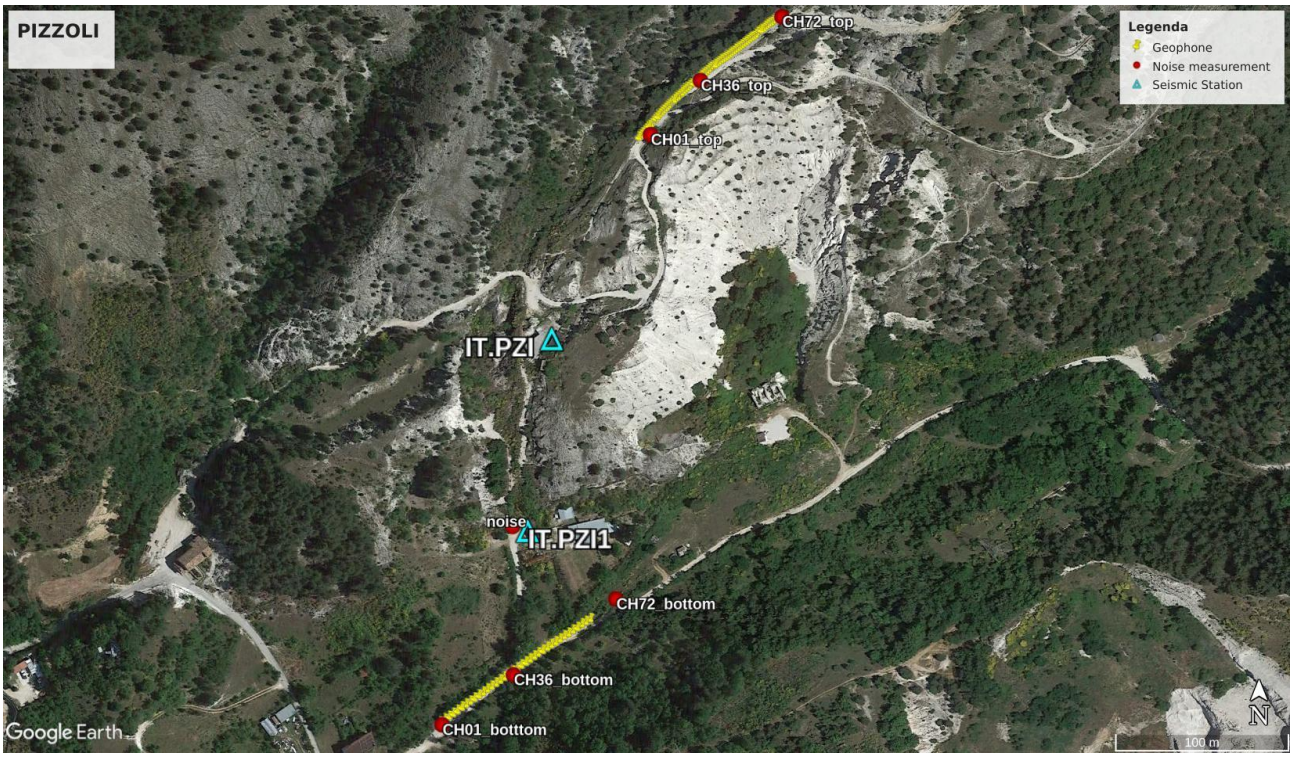

Figure 5. Plan view of the geophysical surveys in proximity of the IT.PZI1 target station (cyan triangle). The previous position of the station (IT.PZI) is also shown. The yellow marks show the linear array of 4.5 Hz vertical geophones (MASW surveys using 72 geophones with a regular spacing of 1.5 m). The red markers indicate the ambient vibrations measurements (Reftek 130 connected to Lennartz 3d 5s) performed approximately at the begin, middle and end position of the MASW line. Further vibration measurement was carried out very close to IT.PZI1 (named 'noise' in the figure). Image from Google Earth http://www.earth.google.com.

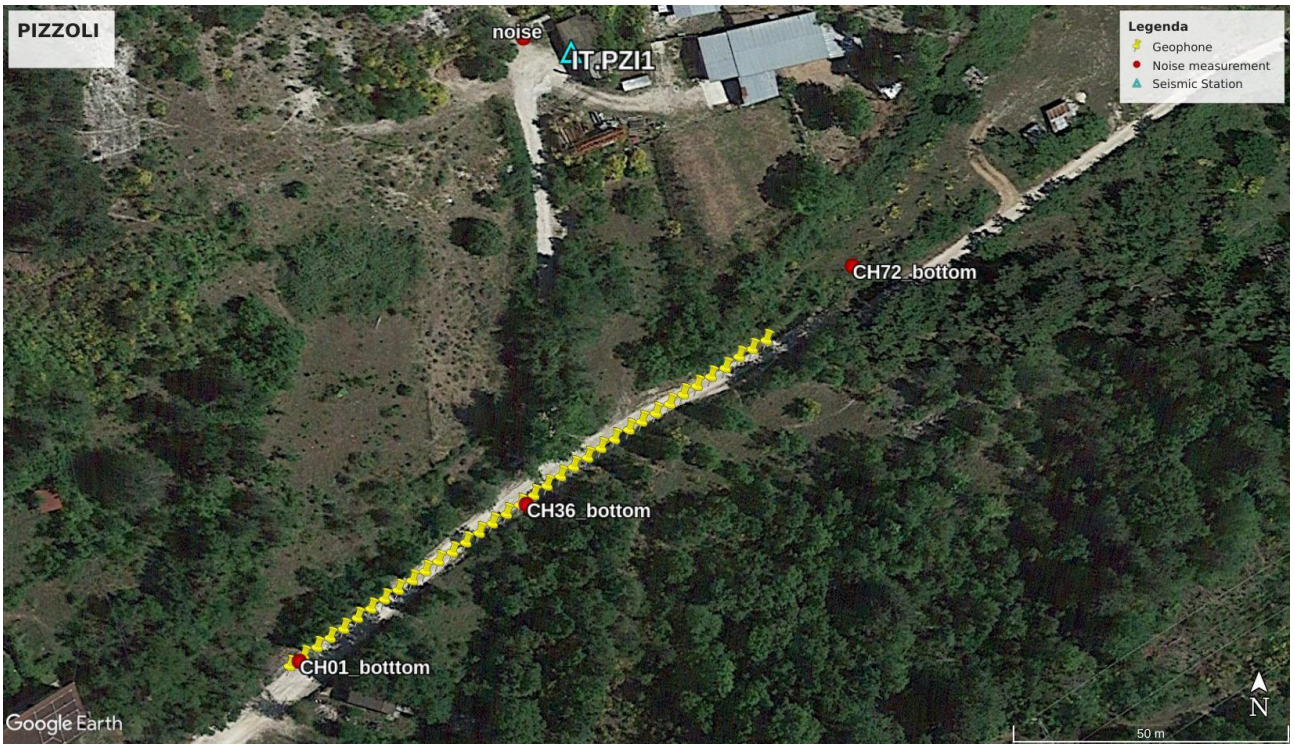

Figure 6. A zoomed view of the geophysical experiment close to IT.PZI1. The linear array of vertical geophones (yellow markers) is also indicated as bottom MASW in this report. Image from Google Earth http://www.earth.google.com.

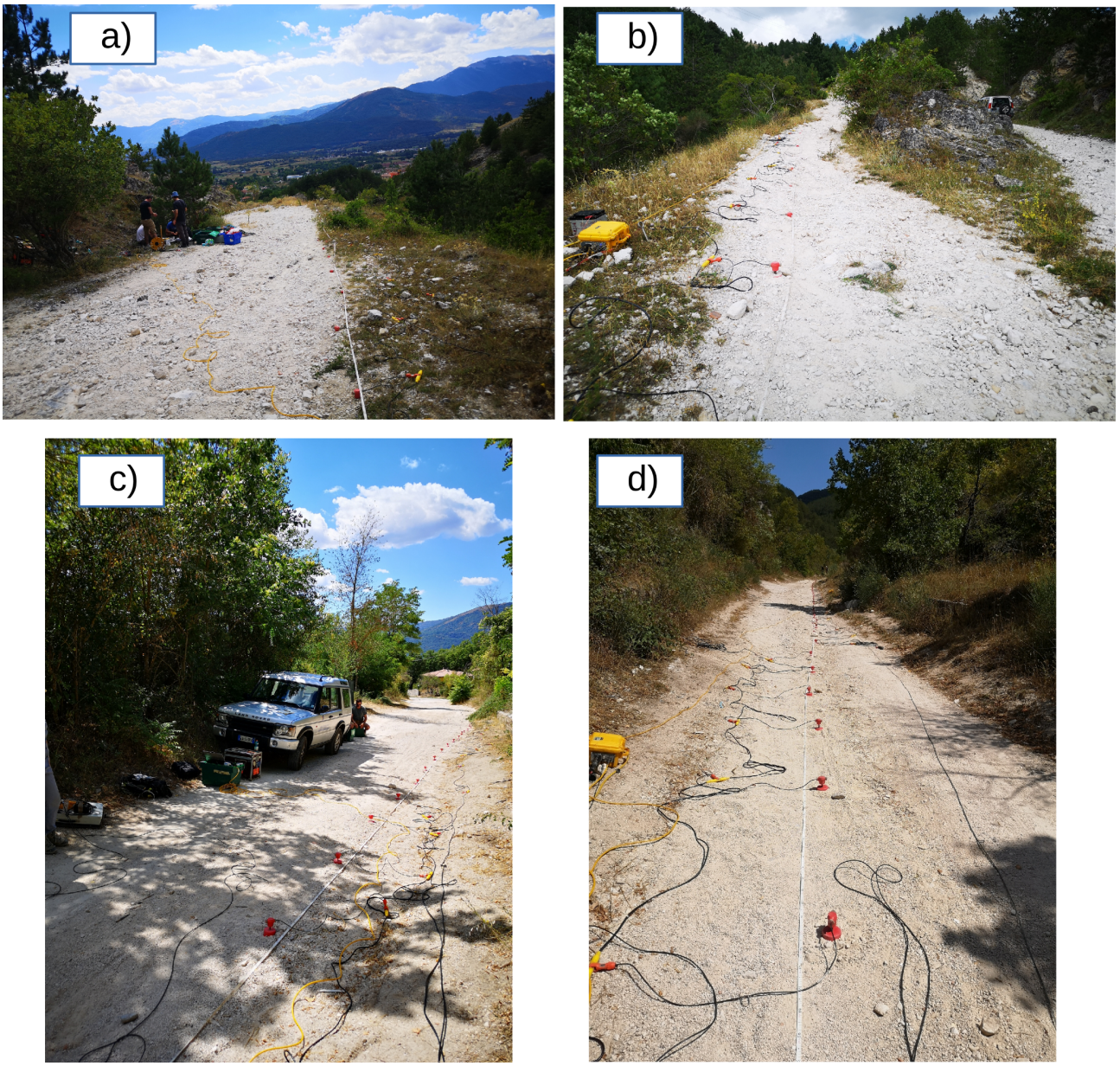

Figure 7. Pictures of the top (a and b) and bottom (c and d) MASW surveys. Panels (a) and (c) refer to the begin part of the MASW line; the panels (b) and (d) show the end part of the line.

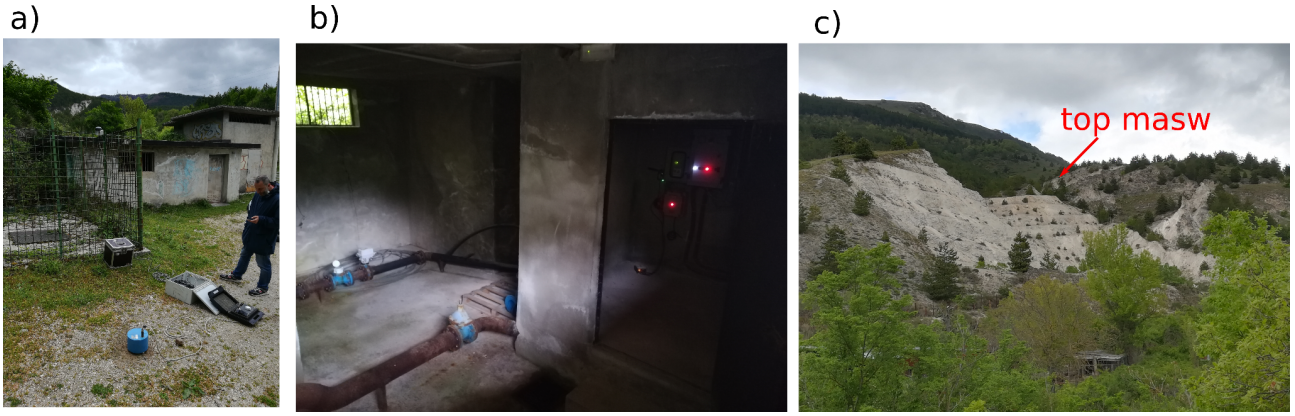

Figure 8. a) Seismic noise measurement close to IT.PZI housing ('noise' mark in Fig. 6). b) Interior of the IT.PZI1 cabinet with detail on the water pipeline. c) Picture taken from the bottom MASW line toward the top MASW line.

1.2 H/V spectral ratio from temporary seismic noise measurements

Figure 9 shows the actual H/V noise curves for the seismic stations installed in the field: points CH01, CH36 and CH72 within the top and bottom MASW line (see Fig. 5), and the closest noise measurement to IV.PZI1 (see Fig. 8a). In general there is not a good agreement of the H/V shapes in the area; the most pronounced peaks are observed on the top MASW line (Fig. 9a) and in particular on the CH72 site (H/V peak with amplitude level around 4 at 0.9 Hz). Noise measurements within the bottom MASW line are characterized by no clear peaks, even if the uncertainties are relatively high (Fig. 9b) and a peak at 0.8-0.9 Hz can be dubitatively recognized as fundamental resonance (f0). The closest 'noise' measurement to IV.PZI1 (Fig. 9c) shows multiple peaks with similar weak amplitude up to 10 Hz (specifically peaks can be recognized at 0.8 Hz, 1.5 Hz, 2.2 Hz, 2.7 Hz and 3.9 Hz). More pronounced peaks are observed in the H/V curve of Fig. 9c at higher frequencies (i.e. between 10 and 20 Hz). The Fourier Amplitude Spectra and directional H/V ratios confirm the presence of multiple peaks but without a clear indication of a narrow resonance frequency.

Note that the H/V curve present in Engineering Strong Motion archive (ESM https://esm-db.eu/; Luzi et al. 2020) at the moment of writing this report is derived from spectral ratios of response spectra computed on 16 earthquakes with magnitude ranging from 3.1 to 4.7 (Fig. 10). Interestingly the 1.6 Hz peak reported in the ESM archive is similar to one found in our noise analysis. However, ESM indicates this H/V curve as broad-band type, i.e. without any clear resonance peak.

To conclude and for the above discussion, from the available data we consider the H/V curve of IV.PZI1 as a broad-band curve without any clear indication of f0.

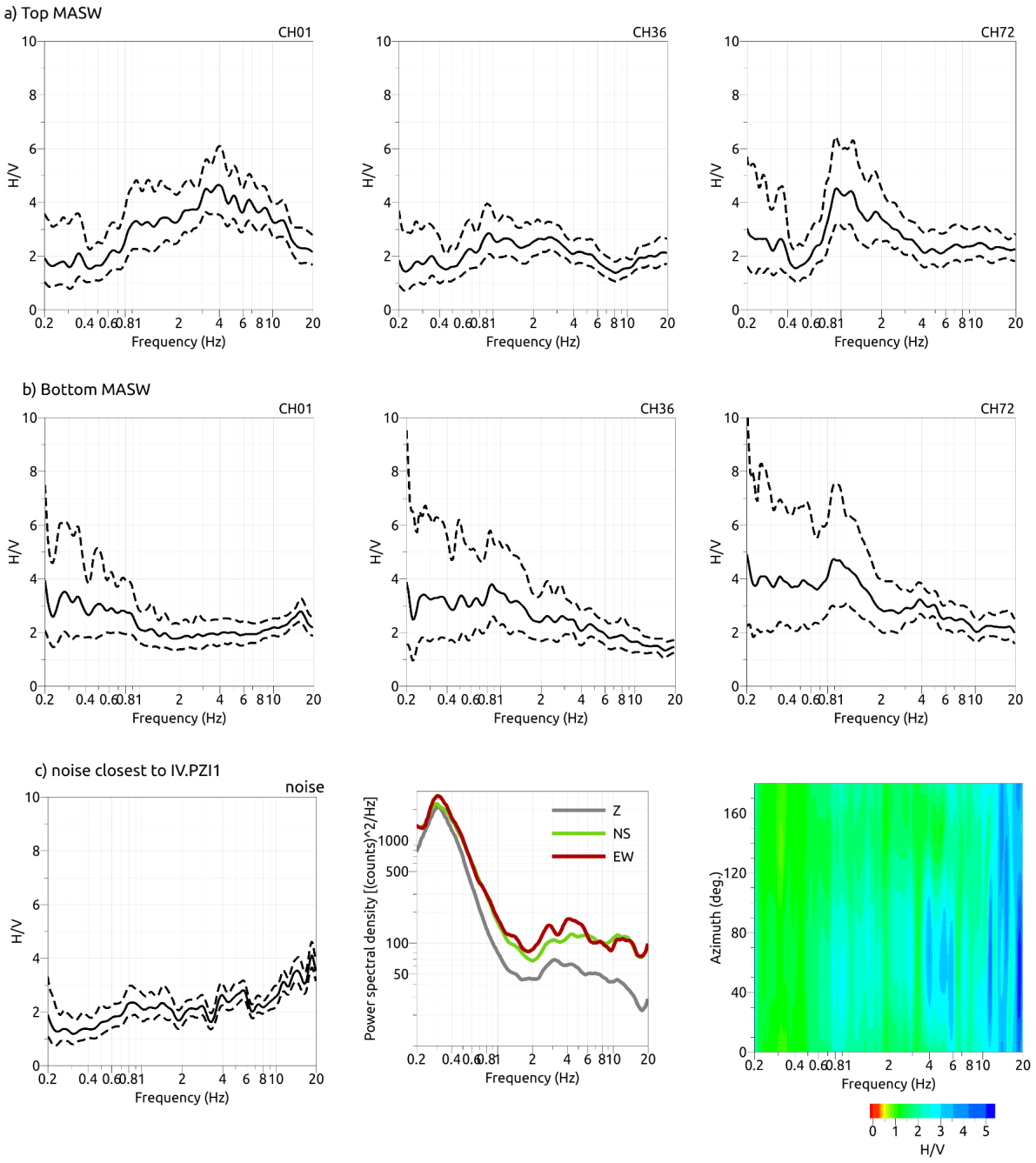

Figure 9. H/V noise spectral ratios (the dashed curves are the mean plus/minus one standard deviation) are reported for the top (a) and bottom (b) MASW surveys. Their positions are indicated in Fig. 5 as CH01, CH36 and CH72. Panel c shows the H/V curves of the closest noise measurement to IT.PZI1 (10 m far; see Fig. 8a). For this measurement, Fourier amplitude spectra of the horizontal (EW and NS) and vertical (Z) components are also given, together with the directional H/V curve (the color scale is proportional to the amplitude value of the H/V curves).

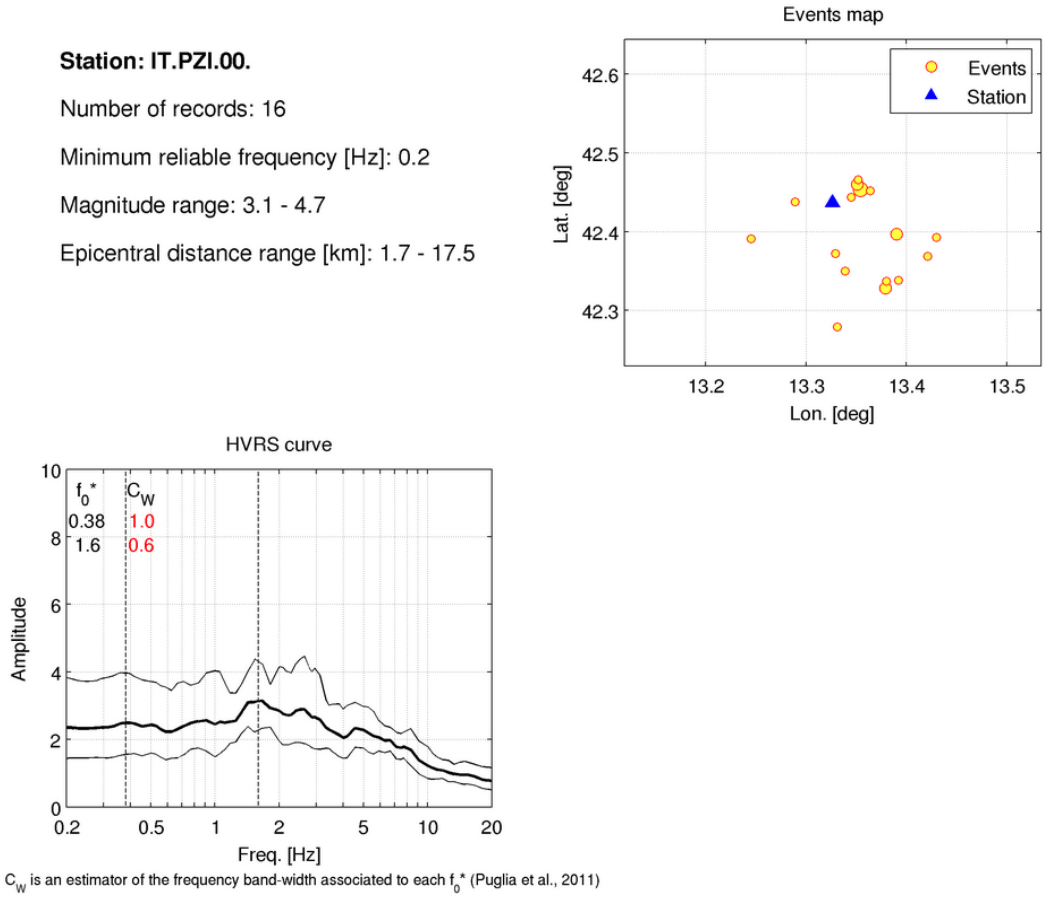

Figure 10. H/V spectral analysis computed on 16 earthquakes redrawn from ESM archive (https://esm-db.eu/). The H/V curve type is indicated by ESM as a broad-band curve.

1.3 Linear Array analysis

The active data acquired using the shots of the hammer in the top and bottom linear array of geophones of Fig. 5 were processed for extracting the surface-wave dispersion (DC) by applying frequency-wavenumber (FK) analysis as implemented in the *GEOPSY* software tools (www.geopsy.org; Wathelet et al. 2020). The passive data recorded on the same linear arrays of geophones were analyzed using the Cross-Correlation technique (Vassallo et al. 2019).

1.3.1 F-K analysis on active data

Figure 11 shows the results obtained by linear F-K analysis on the active data of the top MASW line (see position in Fig. 5). The top MASW line should be indicative of the previous IT.PZI station (operative up to 2013-10-14), which is placed at a distance of about 160 m in south-west direction (Fig. 5). A fairly clear dispersion curve (from 20 Hz up to 60 Hz) is obtained in Fig. 11 for all the shots, with apparent mean phase-velocities ranging from 550-700 m/s (around 20 Hz) and 320-600 m/s (around 60 Hz).
The black lines in Fig. 11 are obtained as manual picking on the stack image and represent the final dispersion curve for each offset. To have a larger clarity in the comparison, the DCs are reported in Figure 12 evidencing larger velocities of the top MASW line in the northern-eastern part rather than in the southern-western portion. Although further studies are needed to better understand the cause of the observed velocity change, it could be tentatively related to a different property of a cataclastic deposit along the MASW line within a fault zone.

f-k analysis was repeated for the bottom MASW line, which is representative of the target station IT.PZI1 (distance about 60 m, see Fig. 6). Figure 13 shows the dispersion results for each single offset. A summary of the picked DCs is shown in Figure 14; apart an outlier curve (mostly related to the offset in the middle of the line) the DCs are in fairly good agreement with an average DC (in blue(showing velocity values of 780 m/s (at 10 Hz), 620 m/s (at 20 Hz) and 520 m/s (at 60 Hz).

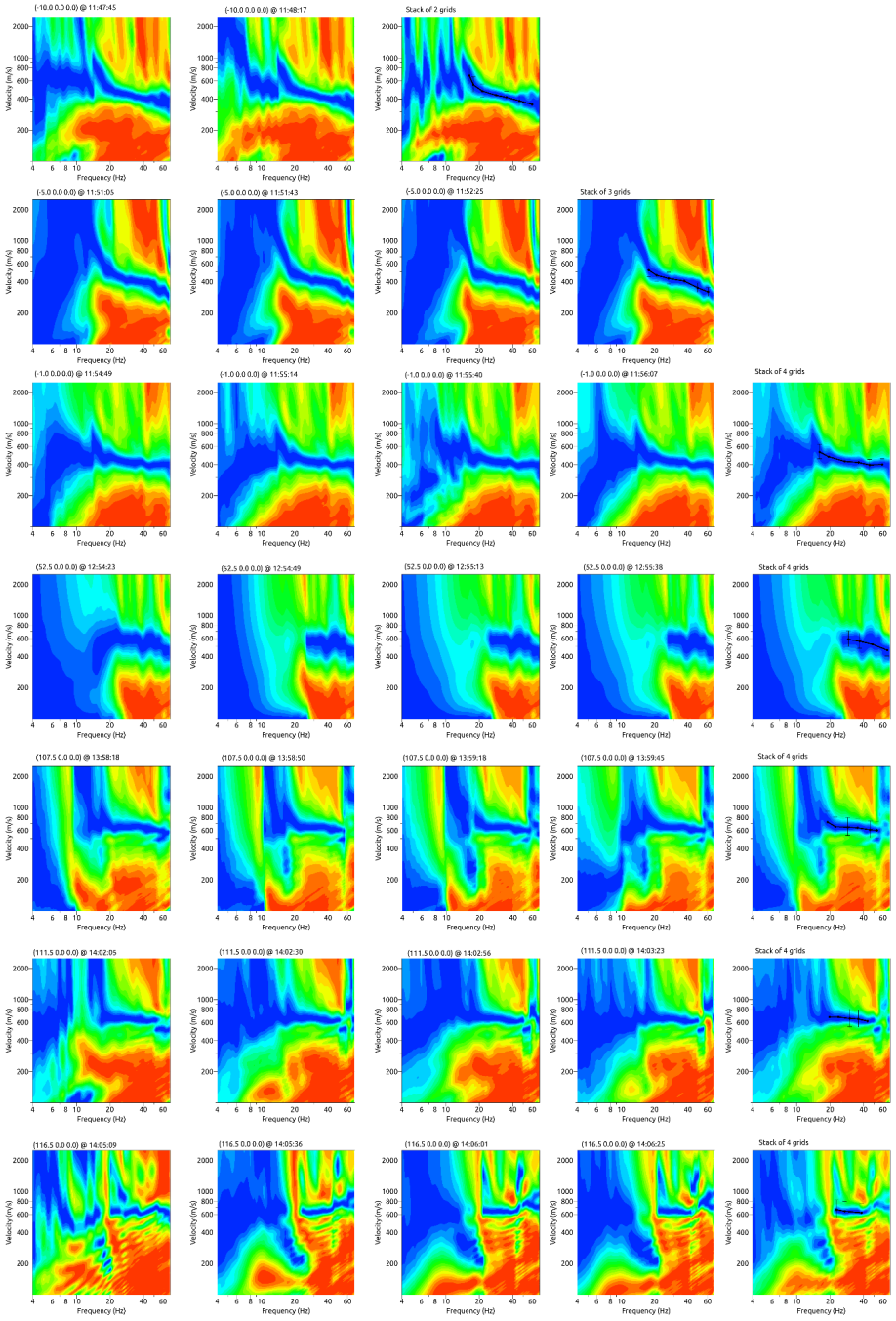

Figure 11. FK analysis on the top MASW line. The results for each single shot are shown; from top to down the offset is -10 m, -5 m, -1 m, 52.5 m , 107.5 m, 111.5 m, 116.5 m (the first and last geophones are considered at a position of 0m and 106.5 m, respectively). Plots in the same horizontal panel refer to the same shot location. The plots in the last column refer to the stack image obtained for the same offset, with the pick curves reported as black lines with vertical bars for taking into account the uncertainties.

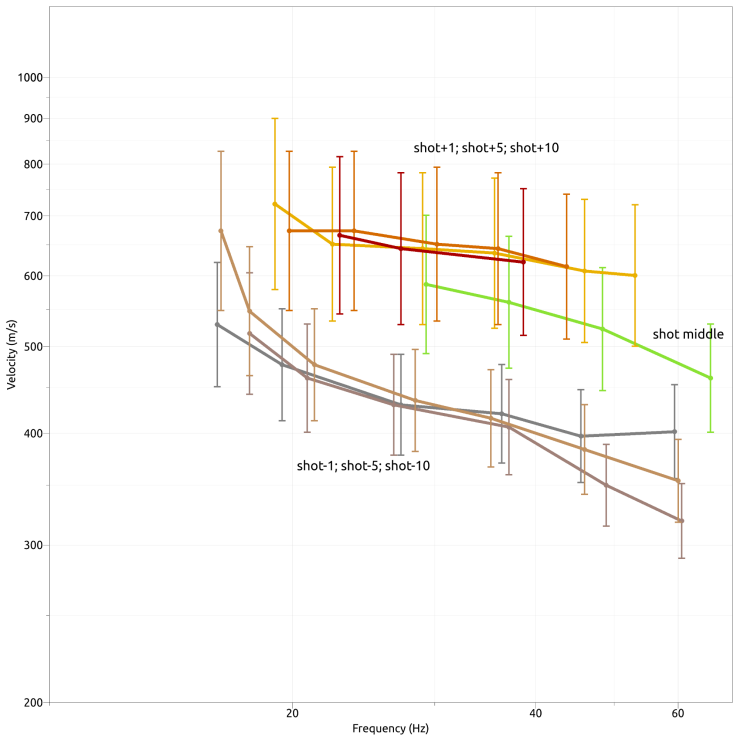

Figure 12. Dispersion curves derived from the F-K analysis of the top MASW line for different shot offsets. The records with offset negative (i.e. shot position at -1m , -5m and -10m from the first geophone considered at 0m) give lower velocities with respect to records with offset positive (i.e +1m, +5m and +10 m from the last geophone considered at 106.5m).

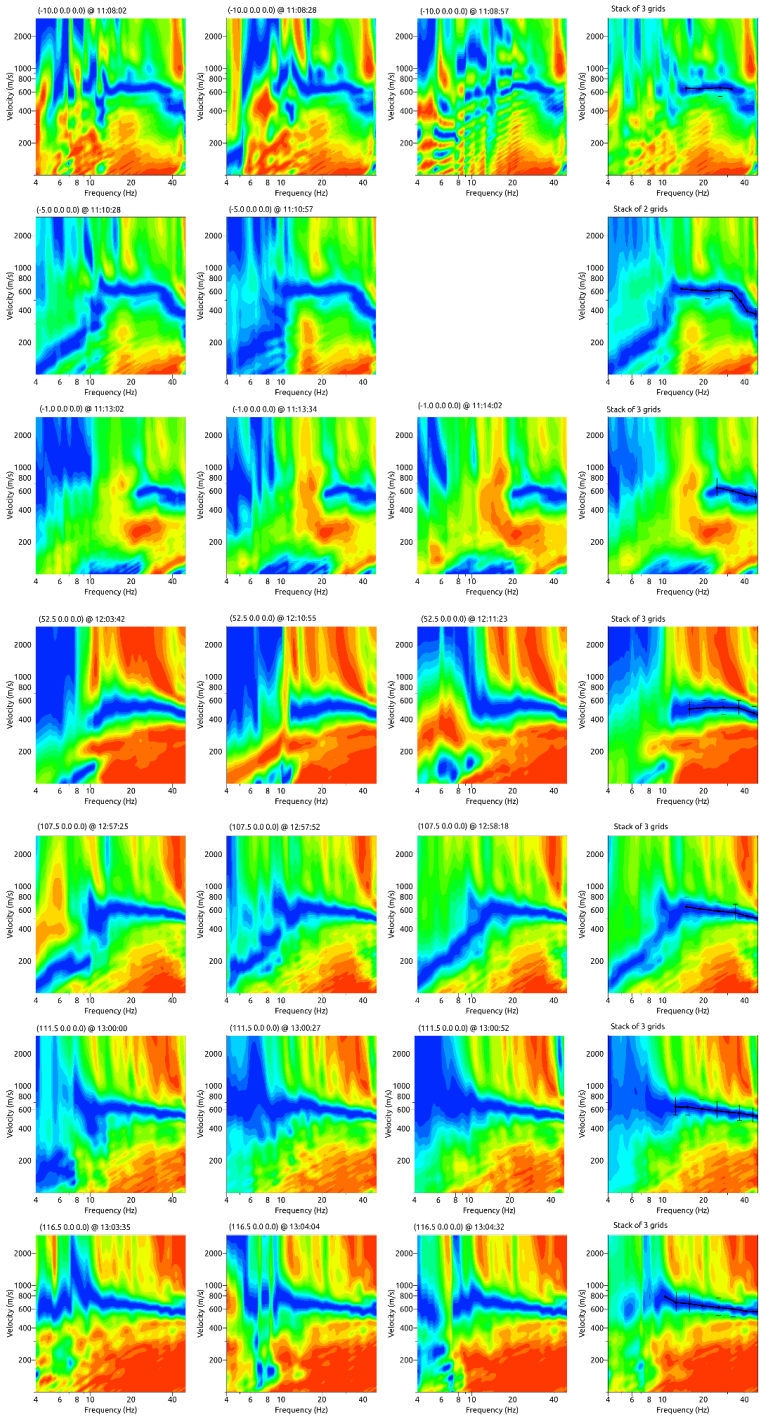

Figure 13. FK analysis on the bottom MASW line (see Fig. 6). From top to down the offset is -10 m, -5 m, -1 m, 52.5 m , 107.5 m, 111.5 m, 116.5 m (the first and last geophones are considered at a position of 0m and 106.5 m, respectively). Plots in the same horizontal panel refer to the same shot location. The plots in the last column refer to the stack image obtained for the same offset, with the pick curves reported as black lines with vertical bars for taking into account the uncertainties.

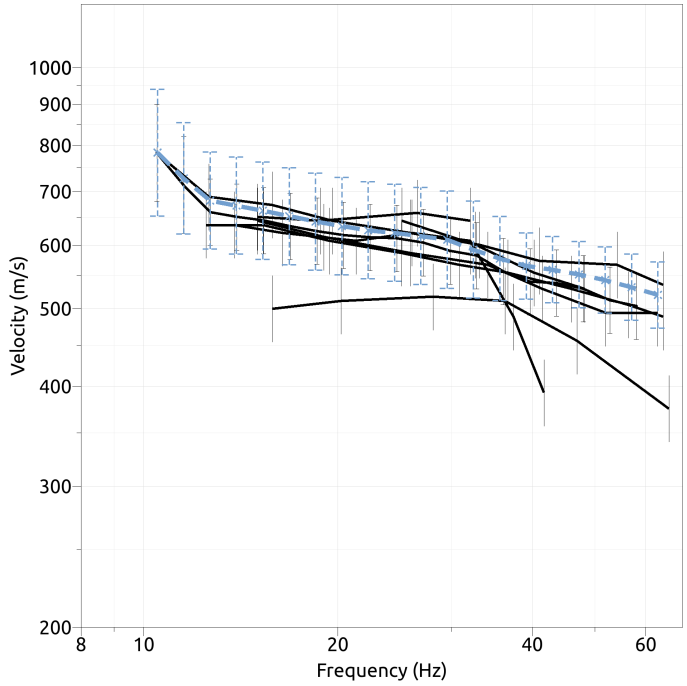

Figure 14. Dispersion curves derived from the F-K analysis of the bottom MASW line for the different shot offset. The average DC among all the offset is shown as the blue one.

1.3.2 Cross-Correlation analysis on passive signals of the bottom line

A Cross-Correlation (CC) method was also applied to the passive data recorded by the bottom linear array of geophones using ad hoc software (Vassallo et. al. 2019). Fig. 15 shows the computed cross-correlations functions (organized according to the distance between station pairs) and the results of the velocity analysis performed on CCs. Specifically, passive data were processed using one-bit normalization and spectral whitening (Bensen et al. 2007). Then, the cross-correlation functions were computed for the processed traces at the different station pairs of arrays (Fig. 15 top panel). To compute the dispersion curve of the seismic signals, we applied a Constant Velocity Stack (CVS) analysis (Yilmaz, 1987) to the CCs functions (Fig. 15 bottom panel). The cross-correlation functions were filtered in different frequency bands starting from 3 to 40 Hz. For each band, the cross-correlation functions were shifted back in time according to different constant velocities starting from 50 m/s until 1500 m/s using a velocity step of 10 m/s. For each frequency band and velocity correction, a Phase-Weighted Stack was computed, and the maximum of the stack function provided the velocity of surface waves at the considered frequency. The dispersion curve (black line in Fig.

15bottom) is automatically identified on the basis of the maximum value of the stack function at each frequency. To compare with the results of the f-k analysis, the average curve of Fig. 14 is also overlaid to the stack image from CC analysis. The DC from f-k analysis is on the lower envelope of the stack image (Fig. 15) slightly underestimating the velocity values from CC, with a difference of the order of 100 m/s. The DC from CC analysis is also characterized by large uncertainties below 10 Hz, we consider the lower limit equal to 6 Hz. Because the two DCs from the f-k and CC analysis are close in the values, we proceed to a further average: the green curve in Fig. 16 is considered in the inversion step.

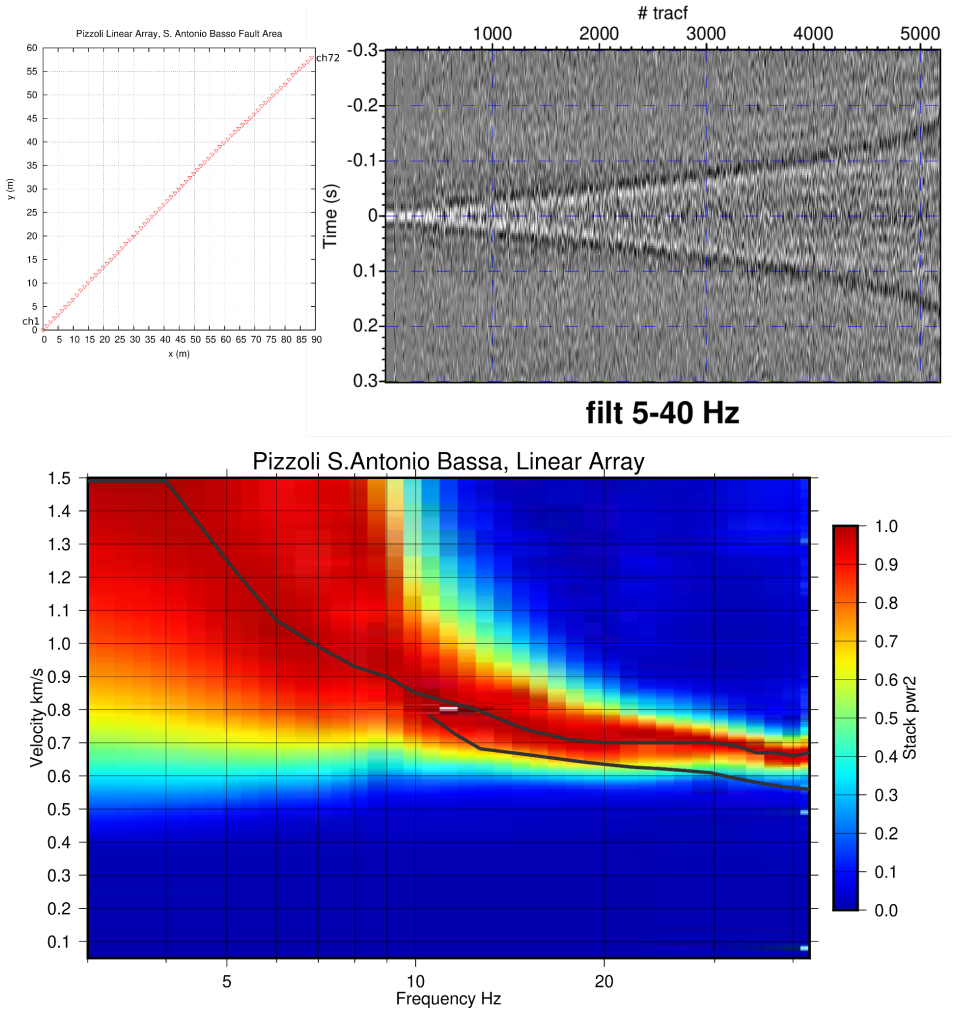

Figure 15. Cross-Correlation (CC) analysis performed on passive data acquired by the bottom linear array of vertical geophones. The top panel shows the geometry of the array, and the CC functions filtered in the frequency band 5-40 Hz. The races in the CC section are organized for increasing interdistance (#tracf). The bottom panel shows the Constant Velocity Stack (CVS) analysis;the black curve follows the maxima of the stack function over frequency. The other black curve overlaid to the Stack is the average dispersion derived from the f-k analysis (i.e. the blue curve of Fig. 14).

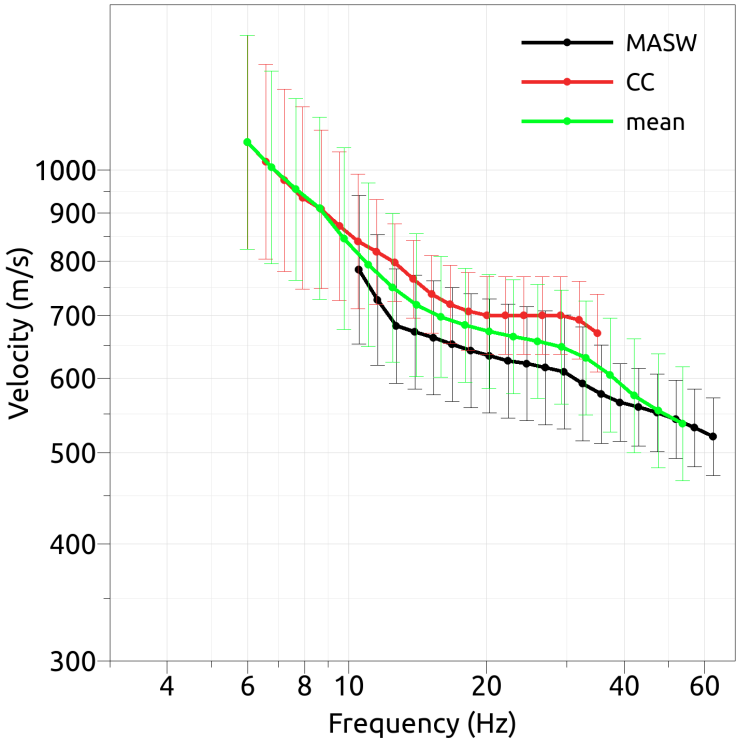

Figure 16. For the inversion step, we considered a dispersion curve (in green) obtained as the average between those derived from f-k active analysis (in black) and the Cross-Correlation passive analysis (in red).

B2. SEISMIC VELOCITY MODEL

To proceed with the inversion step, we considered the average dispersion curve of Fig. 16 (in green) that averages the results from f-k and CC analysis on the bottom line of geophones.

The dispersion curve was associated with the Rayleigh-wave fundamental mode. The models derived from the inversion step (by the *Dinver* tool of Geopsy code; Wathelet et al. 2020) are shown in Fig. 17. We tested several model parameterizations composed of main soft layers over halfspace, including parameterizations that allow a Vs increasing with depth following a linear-law. Based on the available information on the geological structure of the area (see part A of the present report), we found reliable velocity models considering a simple model parameterization of 2 uniform layers over halfspace (Fig. 17). The velocity contrasts are found at depths of about 1.5 m (from 240 m/s to 790 m/s) and 33 meters, where the Vs values increase respectively from 240 to 790 m/s, and from 790 to 1300 m/s.

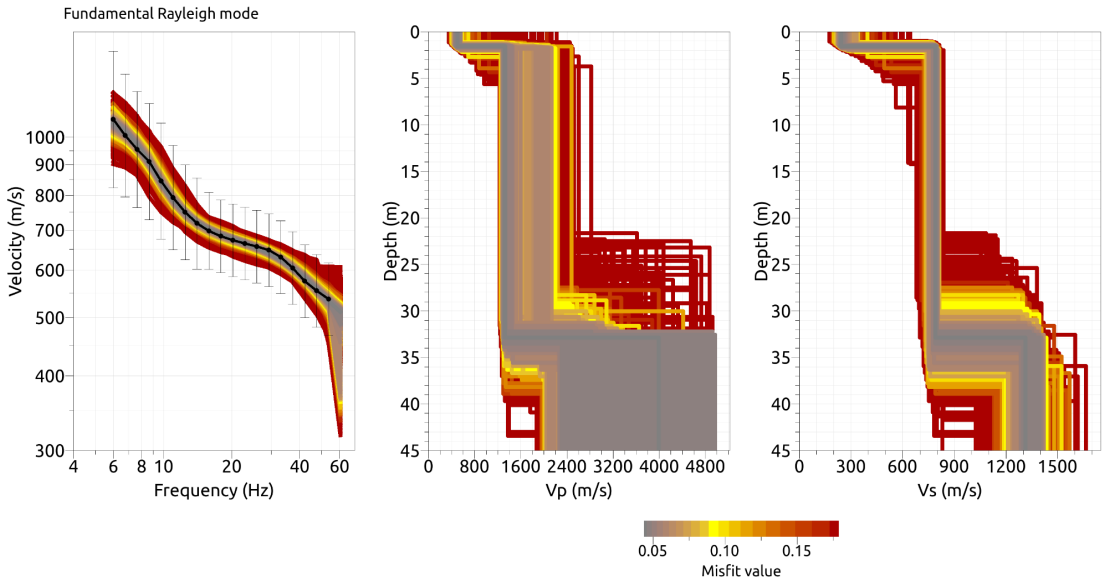

Figure 17. Inversion of the Rayleigh-wave dispersion (field curve is in black colour; the rainbow scale is proportional to the misfit between field and theoretical curves). From right to left) Models of Rayleigh-wave dispersion curves (fundamental mode) are shown together with the compressional (Vp) and shear-wave velocity (Vs) profiles. The best velocity models are presented in Fig. 18.

The layers (from up to bottom) are interpreted consistently with the model proposed in paragraph 5.3 of the Geological part: a very shallow (thick around 2 m) deposit of

colluvium-eluvium over very high fractured rocks of the Pizzoli cataclastic zone with thickness of about 20-40 m. The basement is associated with the carbonatic rocks of the Calcare massiccio Fm.

The best -fit velocity models, extracted from the ensemble of possible solutions by the inversion, are shown in Figure 18 and Table 5.

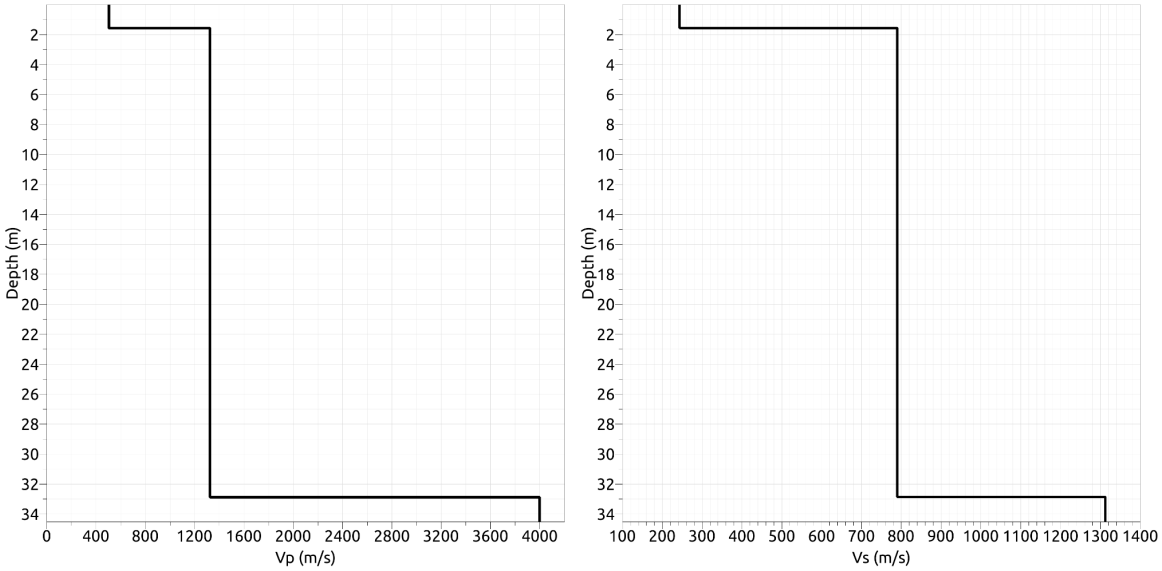

Figure 18. Best Vp and Vs models (extracted from Fig. 17).

Table 5. Best-fit model

From (m)	To (m)	Thickness (m)	Vs (m/s)	Vp(m/s)
0	1.6	1.6	243	505
1.6	32.9	31.3	790	1325
32.9	100	67,1	1313	3997

B3. CONCLUSIONS

Surface-wave analysis at IT.PZI1 station indicates a site of soil class B (Table 6).
HV noise spectral ratios show no clear resonance peaks. The analyses of the linear arrays of vertical geophones provide dispersion curves in the frequency range 6-60 Hz; the inversion of DCs gives the best velocity models of Fig.s 17 and 18 with a bottom layer found at a depth of 33 m (Table 5).
The V_{S30} retrieved from the best inverted model is 707 m/s (Table 6), therefore IT.PZI1 is classified following EC8 and NTC18 as soil class B consistently with the geological information (see the first part of the report). Following the definition of $V_{S,eq}$ within NTC18 and because the layer at Vs > 800 m/s is reached at a depth above 30 m, the $V_{S,eq}$ is equivalent to V_{S30} and the soil class remains B (Table 6). However, the second layer of the best model of Table 5 shows a Vs value very close to 800 m/s, and taking into account the uncertainties on the velocity profile (as shown in Figure 17) the engineering bedrock could be reached at a very shallow depth within 2m (in this case the $V_{S,eq}$ prescribed by NTC18 would be equal to 243 for a soil class C).

Table 6. Soil Class following EC8 and NTC18.

V_{S30} (EC8)	**Soil Class**
707 m/s	B

$V_{S,eq}$ (NTC18)	**Soil Class**
707 m/s	B

ACKNOWLEDGMENTS

We are very grateful to Mai Linh Doan, Stephane Garambois and Christophe Voisin of ISTerre Université Grenoble Alpes for their support during the geophysical surveys.

REFERENCES

Bensen, G.D., Ritzwoller, M.H., Barmin, M.P., Levshin, A.L., Lin, F., Moschetti, M.P., Shapiro, N.M. and Yang, Y., (2007). "Processing seismic ambient noise data to obtain reliable broad-band surface wave dispersion measurements". Geophysical journal international, 169(3), pp.1239-1260.

Blumetti, A. M. (1995). Neotectonic Investigations and Evidence of Paleoseismicity in the Epicentral Area of the January-February 1703, Central Italy. In L. Serva & D. B. Slemmons (Eds.), Perspectives in Paleoseismology (Vol. 7, pp. 83-100): A.E.G. Special Publication.

Carafa, M. M. C., & Bird, P. (2016). Improving deformation models by discounting transient signals in geodetic data: 2. Geodetic data, stress directions, and long-term strain rates in Italy. Journal of Geophysical Research: Solid Earth, 121, 5557-5575. https://doi.org/10.1002/2016JB013038

Carafa, M. M. C., Galvani, A., Di Naccio, D., Kastelic, V., Di Lorenzo, C., Miccolis, S., et al. (2020). Partitioning the ongoing extension of the central Apennines (Italy): fault slip rates and bulk deformation rates from geodetic and stress data. Journal of Geophysical Research: Solid Earth. https://doi.org/10.1029/2019JB018956

Centamore, E., Adamoli, L., Berti, D., Bigi, G., Bigi, S., Casnedi, R., et al. (1991). Carta geologica dei bacini della Laga e del Cellino e dei rilievi carbonatici circostanti (Marche meridionali, Lazio nord-orientale, Abruzzo settentrionale). Studi Geologici Camerti, Volume Speciale 1991/2.

Devoti, R., D'Agostino, N., Serpelloni, E., Pietrantonio, G., Riguzzi, F., Avallone, A., et al. (2017). A Combined velocity field of the Mediterranean Region. Annals of Geophysics, 60(2). GPS; crustal motion; mediterranean.doi:10.4401/ag-7059

EC8: European Committee for Standardization (2004). Eurocode 8: design of structures for earthquake resistance. P1: General rules, seismic actions and rules for buildings. Draft 6, Doc CEN/TC250/SC8/N335.

Galadini, F., & Galli, P. (2000). Active Tectonics in the Central Apennines (Italy) – Input Data for Seismic Hazard Assessment. Natural Hazards, 22(3), 225-268. https://doi.org/10.1023/a:1008149531980

Galli, P. A. C., Giaccio, B., Messina, P., Peronace, E., & Zuppi, G. M. (2011). Palaeoseismology of the L'Aquila faults (central Italy, 2009, Mw 6.3 earthquake): implications for active fault linkage. Geophysical Journal International, 187(3), 1119-1134. 10.1111/j.1365-246X.2011.05233.x

Gruppo di lavoro per la MZS. (2018). Microzonazione Sismica di Livello 3 del comune di Pizzoli (AQ), Regione Abruzzo. Retrieved from https://sisma2016data.it/microzonazione/

Gruppo di Lavoro per la ricostruzione. (2021). Ridefinizione delle Zone di Attenzione delle Faglie Attive e Capaci emerse dagli studi di microzonazione sismica effettuati nel territorio dei Centri abitati di Barete e Pizzoli in provincia de L'Aquila, interessati dagli eventi sismici verificatisi a far data dal 24 agosto 2016. Comuni di Barete-Pizzoli. Retrieved from https://sisma2016data.it/faglie-attive-e-capaci/

Luzi L., Lanzano G., Felicetta C., D'Amico M. C., Russo E., Sgobba S., Pacor, F., & ORFEUS Working Group 5 (2020). Engineering Strong Motion Database (ESM) (Version 2.0). Istituto Nazionale di Geofisica e Vulcanologia (INGV). https://doi.org/10.13127/ESM.2

Moro, M., Bosi, C., Galadini, F., Galli, P., Giaccio, B., Messina, P., & Sposato, A. (2002). Analisi paleosismologiche lungo la faglia del M. Marine (Alta Valle dell'Aterno): risultati preliminari. Il Quaternario, 15, 259-270.

Moro, M., Falcucci, E., Gori, S., Saroli, M., & Galadini, F. (2016). New paleoseismic data across the Mt. Marine Fault between the 2016 Amatrice and 2009 L'Aquila seismic sequances (Central Apennines). Annals of Geophysics, 59.

NTC18: Ministero delle Infrastrutture e dei Trasporti (2018). Aggiornamento delle Norme Tecniche per le Costruzioni. Part 3.2.2: Categorie di sottosuolo e condizioni topografiche, Gazzetta Ufficiale n. 42 del 20 febbraio 2018 (in Italian).

Servizio Geologico d'Italia (Cartographer) (1955). Geological Map of Italy (Sheet 139, L'Aquila, scale 1:100.000)

Technical Commission SM, (2015). Microzonazione sismica. Standard di rappresentazione e archiviazione informatica, Versione 4.0b (Commissione tecnica interistituzionale per la MS nominata con DPCM 21 aprile 2011).

Vassallo, M., De Matteis, R., Bobbio, A., Di Giulio, G., Adinolfi, G.M., Cantore, L., Cogliano, R., Fodarella, A., Maresca, R., Pucillo, S. and Riccio, G. (2019). Seismic noise cross-correlation in the urban area of Benevento city (Southern Italy)" Geophysical Journal international, 217(3), pp.1524-1542.

Wathelet, M., Chatelain, J.L., Cornou, C., Giulio, G.D., Guillier, B., Ohrnberger, M. and Savvaidis, A., (2020). Geopsy: A user-friendly open-source tool set for ambient vibration processing. Seismological Research Letters, 91(3), pp.1878-1889.

Yilmaz O. (1987). Seismic data processing in Investigations in Geophysics, 2: Soc. Expl. Geophys, series Eds., eds Doherty S.M., Neitzel E.B.

Vezzani, L., & Ghisetti, F. (Cartographer). (1998). Carta Geologica dell'Abruzzo, scale 1:100,000

Disclaimer and limits of use of information

The INGV, in accordance with the Article 2 of Decree Law 381/1999, carries out seismic and volcanic monitoring of the Italian national territory, providing for the organization of integrated national seismic network and the coordination of local and regional seismic networks as described in the agreement with the Department of Civil Protection.

INGV contributes, within the limits of its skills, to the evaluation of seismic and volcanic hazard in the Country, according to the mode agreed in the ten-year program between INGV and DPC February 2, 2012 (Prot. INGV 2052 of 27/2/2012), and to the activities planned as part of the National Civil Protection System. In particular, this document[1] has informative purposes concerning the observations and the data collected from the monitoring and observational networks managed by INGV. INGV provides scientific information using the best scientific knowledge available at the time of the drafting of the documents produced; however, due to the complexity of natural phenomena in question, nothing can be blamed to INGV about the possible incompleteness and uncertainty of the reported data.

INGV is not responsible for any use, even partial, of the contents of this document by third parties and any damage caused to third parties resulting from its use. The data contained in this document is the property of the INGV.

This study has benefited from funding provided by the Italian Presidenza del Consiglio dei Ministri - Dipartimento della Protezione Civile (DPC). This paper does not necessarily represent DPC official opinion and policies.

Esclusione di responsabilità e limiti di uso delle informazioni

L'INGV, in ottemperanza a quanto disposto dall'Art. 2 del D.L. 381/1999, svolge funzioni di sorveglianza sismica e vulcanica del territorio nazionale, provvedendo all'organizzazione della rete sismica nazionale integrata e al coordinamento delle reti sismiche regionali e locali in regime di convenzione con il Dipartimento della Protezione Civile.

L'INGV concorre, nei limiti delle proprie competenze inerenti la valutazione della Pericolosità sismica e vulcanica nel territorio nazionale e secondo le modalità concordate dall'Accordo di programma decennale stipulato tra lo stesso INGV e il DPC in data 2 febbraio 2012 (Prot. INGV 2052 del 27/2/2012), alle attività previste nell'ambito del Sistema Nazionale di Protezione Civile. In particolare, questo documento[1] ha finalità informative circa le osservazioni e i dati acquisiti dalle Reti di monitoraggio e osservative gestite dall'INGV. L'INGV fornisce informazioni scientifiche utilizzando le migliori conoscenze scientifiche disponibili al momento della stesura dei documenti prodotti; tuttavia, in conseguenza della complessità dei fenomeni naturali in oggetto, nulla può essere imputato all'INGV circa l'eventuale incompletezza ed incertezza dei dati riportati.

L'INGV non è responsabile dell'utilizzo, anche parziale, dei contenuti di questo documento da parte di terzi e di eventuali danni arrecati a terzi derivanti dal suo utilizzo. La proprietà dei dati contenuti in questo documento è dell'INGV.

Lo studio presentato ha beneficiato del contributo finanziario della Presidenza del Consiglio dei Ministri - Dipartimento della Protezione Civile; la presente pubblicazione, tuttavia, non riflette necessariamente la posizione e le politiche ufficiali del Dipartimento.

[1]This document is level 3 as defined in the "Principi della politica dei dati dell'INGV (D.P. n. 200 del 26.04.2016)"

GENERAL INFORMATION

Authors	Institutions	Contacts [email]	Compiling date [DD/MM/YY]
Di Giulio Giuseppe	INGV	giuseppe.digiulio@ingv.it	11/12/2021

Station description

Station name	Network code	Latitude [WGS84]	Longitude [WGS84]	Sensor depth [m]
PZI1	IT	42.4356	13.3262	At ground level

Site characterization summary

Indicators					
fo +/ std [Hz]	Value	none	Quality index Qi1		
	References	see this report			
	URL of report				
Velocity profiles [YES/NO]	Value	YES	Quality index Qi1	1	
	References				
	URL of report				
Vs30 +/ std [m/s]	Value	707	Quality index Qi1	1	
	References				
	URL of report				
Surface geology [short description]	Value	Very fractured rock	Quality index Qi1	1	
	References	see this report			
	URL of report				
Seismological bedrock depth +/ std [m]	Value	33	Quality index Qi1	0.67	
	References				
	URL of report				
Site class EC8	Value	B	Quality index Qi1	1	
	References				
	URL of report				
Engineering bedrock depth +/ std [m]	Value	33	Quality index Qi1	1	
	References				
	URL of report				

Distance from the seismic station [m]		Final quality index (Final_QI)	Comments
min	min		
10	300	0.56	QI2= 0.72; QI3=0.4. QI3 value suffers of the null value of f0

RESONANCE FREQUENCY

fo +/ STD [Hz]	none
Quality index 1	

Source	Earthquake		Ambient noise	✔

Ambient noise

Method	H/V	✔	Ellipticity		Other	
fo +/ std [Hz]	none					

Experiment date [DD/MM/YY]	Distance from station [m]	Lat. [WGS84]	Lon. [WGS84]
19/05/2021	10	44.921415	11.875428

Environment

Weather conditions	Sunny	Windy	Rain
			✔
Soilsensor coupling	**Earth**	**Asphalt**	**Artificial**
	✔		
Urbanization	**None**	**Dense**	**Scattered**
			✔

Equipment

Sensor	Type [acc/vel]	manufacturer	cutoff frequency [Hz]
	vel	Lennartz	0.2
Digitizer	**Type**	**Manufacturer**	**Sampling frequency [Hz]**
	130	Reftek	250
Measurement	**Number**	**Duration [min]**	
	1	60	

Analysis

Software	geopsy
Smoothing type (e.g. triangular, KonnoOhmachi, ...)	**Window length [s]**
K-O	60

Fo uncertainty estimate from

Fo from individual windows	H/V curve width	Manual picking

Earthquake

Method	HVSR		SSR		GIT		Other	
fo +/ std [Hz]								

Recording period [DD/MM/YY]		Number of earthquakes
from	to	

Epicentral distance [km]		Magnitude range	
from	to	from	to

HVSR

Seismic phase	P	S	Coda	S + coda	All

window duration [s]	Min	Max

SSR

Seismic phase	P	S	Coda	S + coda	All

Reference station	Lat. (WGS84)	Lon. (WGS84)

window duration [s]	Min	Max

GIT

Parameters	Free (to be inverted)	Imposed
Reference paper		

Reference station	Lat. (WGS84)	Lon (WGS84)

Contacts: Cecile.Cornou@univgrenoblealpes.fr Giovanna.Cultrera@ingv.it Giuseppe.Digulio@ingv.it

Vs30

Vs30 +/ STD [m/s]	707 +/- 100
Quality index 1	1

Source	Geophysical measurements	✔	Geotechnical measurements		Digital Elevation Model (DEM)		Geology		DEM & Geology	

Geophysical measurements

Method	Surface waves methods (active, passive methods)		Borehole methods (DH, CH, PS Logging)	
Vs30 +/ STD [m/s]	From Vs(z)	✔	From DownHole	
	From Vr40		From CrossHole	
	From VszVs30 correlation		From PS Logging	
Reference relationship Vsz Vs30				

Geotechnical measurements

Method	NSPT		CPT		Shear strength		OTHER	
Vs30 +/ STD [m/s]								

Experiment date [DD/MM/YY]	Distance from station [m]	Lat. [WGS84]	Lon. [WGS84]

Reference relationship Vs30geotechnical parameter	
	N-SPT
	CPT
	Shear strength
	Other

Geology

Method	Geological map		Stratigraphic log	
Vs30 +/ STD [m/s]				
Geological map scale				
Geological unit name				
Stratigraphic log	Experiment date [DD/MM/YY]		Lat. [WGS84]	Lon. [WGS84]
Reference relationship Vs30geology				
Reference relationship Vs30Stratigraphic log				

Digital Elevation Model

Vs30 +/ STD [m/s]				
DEM resolution		Slope range (degree)	from	
			to	
Reference relationship Slope Vs30				

DEM & Geology

Vs30 +/ STD [m/s]	
Reference relationship Slope Vs30 geology	

Contacts: Cecile.Cornou@univgrenoblealpes.fr Giovanna.Cultrera@ingv.it Giuseppe.Digulio@ingv.it

Vs profile

Quality index 1	1

Source

Noninvasive methods (active and/or passive seismics)			
Active surface waves	✔	Refraction	
Passive surface waves	✔	Refection	
HV / ellipticity			

Invasive methods (measurement in borehole)	
Cross-hole / Down-hole	
Geotechnical methods (CPT, SPT, ...)	
PS-Logging	

Noninvasive : surface waves methods

Experiment date [DD/MM/YY]	Distance from station [m]		Lat. [WGS84] center location	Lon. [WGS84] center location
	Min	Max		
19/08/2020	60	150	42.4356	13.3262

Active surface waves acquisition layout

Minimum receiver spacing (m)	1.5
Profile length (m)*	106.5
Geophones number	72
Number of profiles	1

** Provide the length for the various profiles (e.g. 46 m, 94 m)*

Geophone cut-off frequency (Hz)	4.5
Geophone type (vertical / horizontal)	vertical
Geophone manufacturer	Geospace
Source (hammer, vibrator, ...)	hammer
Digitizer type	Geode
Digitizer manufacturer	Geometrics

Weather conditions	Sunny	Windy	Rain	Soilsensor coupling	Earth	Asphalt	Artificial	Urbanization	None	Dense	Scattered
	✔						✔				✔

Passive surface waves acquisition layout

Number of sensors	
Minimum array aperture	1.5
Maximum array aperture	106.5
Number of arrays	1
Minimum duration [min]	120

Sensor cut-off frequency (Hz)	4.5
Sensor type (vertical / horizontal)	vertical geophones
Sensor manufacturer	Geospace
Digitizer type	Geode
Digitizer manufacturer	Geometrics

Weather conditions	Sunny	Windy	Rain	Soilsensor coupling	Earth	Asphalt	Artificial	Urbanization	None	Dense	Scattered
	✔						✔				✔

Type of dispersion and/or H/V estimates

		Reference paper (Name, Journal, DOI)
Rayleigh DC	✔	www.geopsy.org (FK on linear array of geophones and CC analysis)
Love DC		
Ellipticity		
H/V (DFA, EHVR)		
H/V (SH)		

Dispersion curves

	Rayleigh	*Love*
Min wavelength (m)	8 (R0)	
Max. wavelength (m)	180 (R0)	
Min. phase vel. (m/s)		
Max. phase vel. (m/s)		
Modes (R0, L0, ...)		

H/V or Ellipticity curves

Min. frequency (Hz)	Max. frequency (Hz)

Inversion

Rayleigh waves		Love waves		Ellipticity curves		H/V (DFA, EHVR)		H/V (SH)		resonance frequency	

A priori information used in inversion	seismic refraction		stratigraphic log		geotechnical information		water table depth	

Inversion algorithm/code	dinver (geopsy code)
Reference	www.geopsy.org

Contacts: Cecile.Cornou@univgrenoblealpes.fr Giovanna.Cultrera@ingv.it Giuseppe.Digulio@ingv.it

Noninvasive : body waves methods

Experiment date [DD/MM/YY]	Distance from station [m]		Lat. [WGS84] center location	Lon. [WGS84] center location
	Min	Max		

Acquisition layout

Receiver spacing (m)	
Profile length (m)*	
Geophones number	
Number of profiles	
Shot spacing (m) - reflection meas.	

Geophone cut-off frequency (Hz)	
Geophone type (vertical / horizontal)	
Geophone manufacturer	
Source (hammer, vibrator, ...)	
Digitizer type	
Digitizer manufacturer	

** Provide the length for the various profiles (e.g. 46 m, 94 m)*

Weather conditions	Sunny	Windy	Rain	Soilsensor coupling	Earth	Asphalt	Artificial	Urbanization	None	Dense	Scattered

Processing methods

		Reference paper (Name, Journal, DOI)
classical refraction		
refraction tomography		
classical reflection		
advanced method		

Invasive methods

	DownHole	CrossHole	PSLogging	SPT	CPT	OTHER
Borehole depth (m)						
Geophone type						
Source type						
Distance between wells						
Depth resolution (m)						
Latitude (WGS84)						
Longitude (WGS84)						
Distance from station (m)						
P-wave velocity						
S-wave velocity						

Processing methods

		Reference paper (Name, Journal, DOI) or ASTM norm
Down-Hole		
Cross-Hole		
PS-Logging		
SPT		
CPT		
OTHER		

Authoritative velocity profile

Note: You do not have to fill in all the columns. You can provide either single values for Vp or Vs (e.g. profiles derived from borehole measurements) or either a range for Vp and Vs (e.g. profiles derived from stochastic surface waves inversion)

Is Vs derived from Vp ?	**Yes**		**No**	✔

Top depth (m)	Bottom depth (m)	Vp (m/s)	STD Vp (m/s)	Vs (m/s)	STD Vs (m/s)	Vs range		Vp range	
						Vs min (m/s)	Vs max (m/s)	Vp min (m/s)	Vp max (m/s)
0	1,6	505		243					
1,6	32,9	1325		790					
32,9	-	3997		1313					

Figure with authoritative velocity profiles

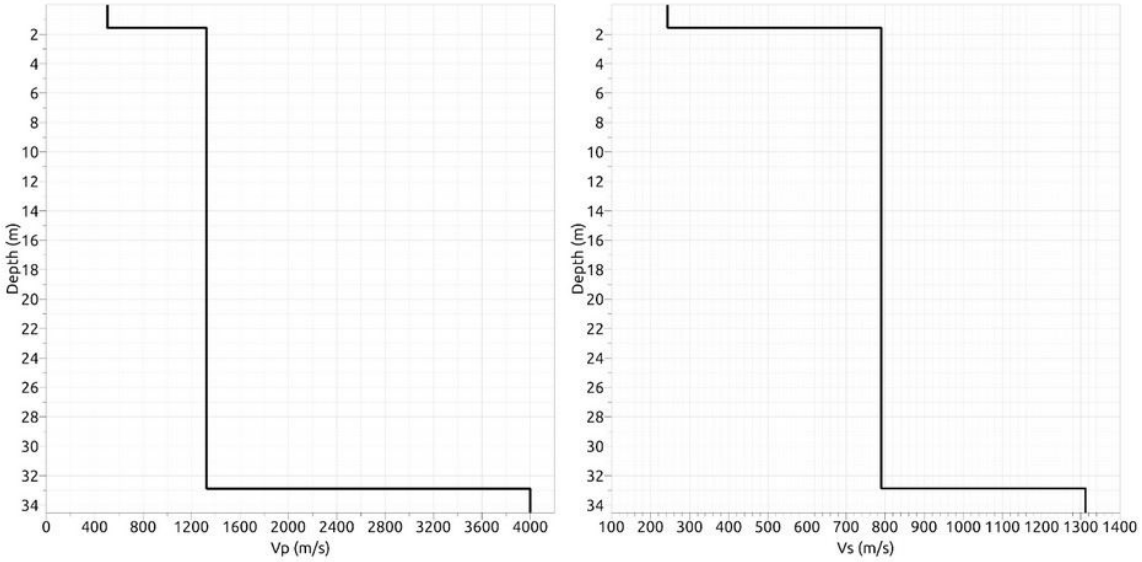

Surface geology

Quality index 1	1

Source	Cartography (geological, lithological, ...)	✔	Field survey	✔	Stratigraphic log	

Geological map

Map reference	Carta geomorfologica dei comuni Barete-Pizzoli (AQ) at 1:5:000 – FAC	
Map scale	1:5000	
Map sheet		
Predominent geologic/lithologic unit	Name :	Masa
	Description :	
	Age :	
	Thickness :	
	Rock mass structure :	
Fault presence	✔	
Weathering	✔	
Crosssection		

Field survey

Map reference		
Map scale		
Predominent geologic/lithologic unit	Name :	
	Description :	
	Age :	
	Thickness :	
	Rock mass structure :	
Fault presence		
Weathering		
Crosssection		

Stratigraphic log

log depth (m)	

Top depth (m)	Bottom depth (m)	Stratigraphic description

Contacts: Cecile.Cornou@univgrenoblealpes.fr Giovanna.Cultrera@ingv.it Giuseppe.Digulio@ingv.it

Surface geology

Map

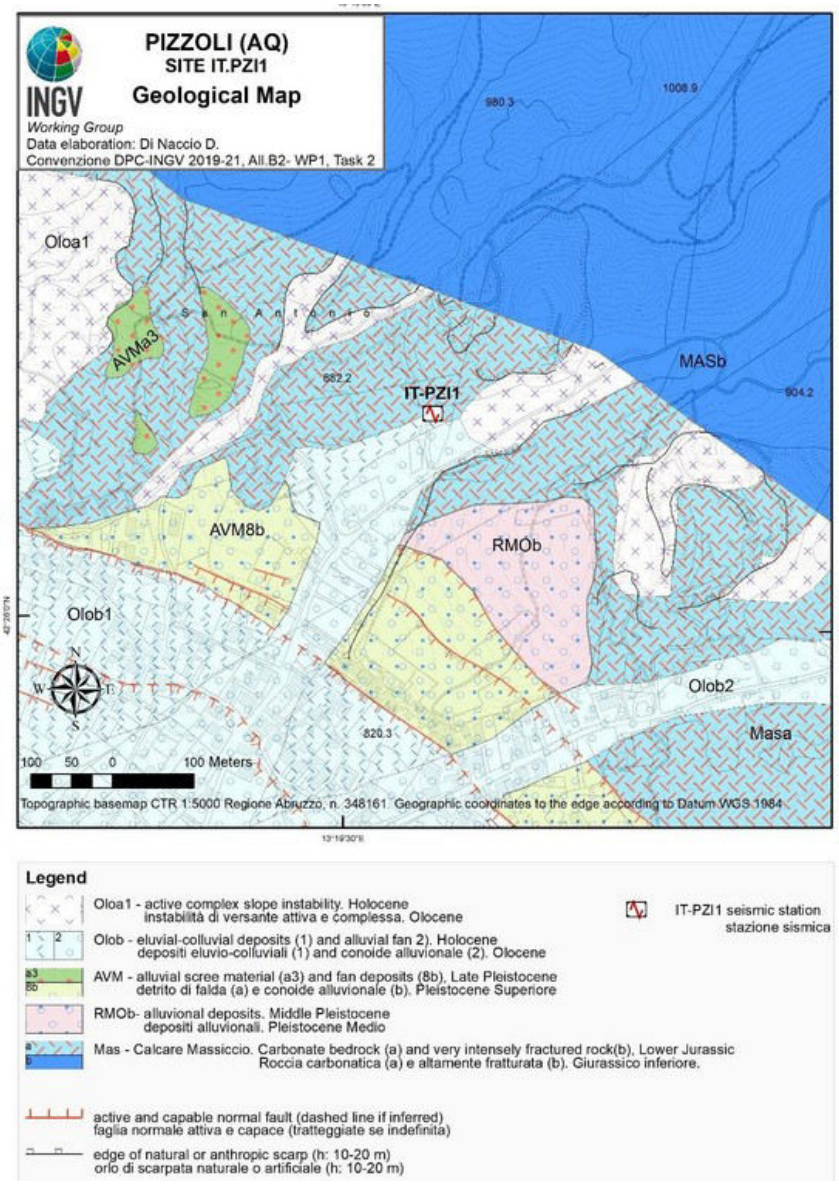

Contacts: Cecile.Cornou@univgrenoblealpes.fr Giovanna.Cultrera@ingv.it Giuseppe.Digulio@ingv.it

Site class

Site class	B
Quality index 1	1

Reference building code for site classification (EC81, EC82, NEHRP, national code, ...)	EC8, NTC18

Source	Geophysical measurements	✔	Geotechnical measurements		Digital Elevation Model (DEM)		Geology		DEM & Geology	

Reference relationship geology soil class	
Reference relationship slope from DEM soil class	
Reference relationship slope from DEM geology soil class	

Parameters for deriving soil class as prescribed in building code	VS30, VSEQ

Contacts: Cecile.Cornou@univgrenoblealpes.fr Giovanna.Cultrera@ingv.it Giuseppe.Digulio@ingv.it

Seismological bedrock depth

Depth +/ STD [m]	33 +/- ?
Quality index 1	0,67

Source	Vs profiles	✔	Geology		Other (gravity, seismic refraction, TDEM, ...)	
	Resonance frequency		Stratigraphic log			

Vs profile

	Noninvasive methods	Invasive seismic methods	Geotechnical methods
Bedrock depth +/ STD(m)	33 +/- ?		
Bedrock Vs +/ STD(m)	33 +/- ?		
Bedrock Vp +/ STD(m)	33 +/- ?		
Is Vs derived from Vp ?	Yes		No ✔

Resonance frequency

Bedrock depth +/ STD(m)	
Reference relationship Fo bedrock depth	

Geology

Bedrock depth +/ STD(m)	
Bedrock geological unit	carbonatic rocks
Reference	see report

Stratigraphic log

Bedrock depth +/ STD(m)	
Bedrock geological unit	
Reference	

Other methods

	Bedrock depth +/ STD(m)	Reference
Gravity		
Seismic refraction		
Seismic reflection		
TDEM		

Contacts: Cecile.Cornou@univgrenoblealpes.fr Giovanna.Cultrera@ingv.it Giuseppe.Digulio@ingv.it

Engineering bedrock depth

Depth +/ STD [m]	33 +/- **
Quality index 1	1

Reference Vs related to engineering bedrock in m/s		Reference building code for site classification (EC81, EC82, NEHRP, national code, ...)	EC8, NTC18

Source	Vs profile	✔	Geology		Stratigraphic log	

**See the report: The second layer 2m deep shows Vs of 790 m/s; the engineering bedrock could be more superficial

Vs profile

	Noninvasive methods	Invasive seismic methods	Geotechnical methods
Bedrock depth +/ STD(m)	33 + ?		

Is Vs derived from Vp ?	Yes		No	✔

Geology

Bedrock depth +/ STD(m)	
Bedrock geological unit	
Reference	

Stratigraphic log

Bedrock depth +/ STD(m)	
Bedrock geological unit	
Reference	

Contacts: Cecile.Cornou@univgrenoblealpes.fr Giovanna.Cultrera@ingv.it Giuseppe.Digulio@ingv.it